

INVESTIGATION OF THE OPTICAL PROPERTIES OF THE NANO-STRUCTURE BASED TIN-OXIDE SEMICONDUCTORS

HULUMTIMI I VETIVE OPTIKE TË GJYSMËPËRÇUESVE PREJ OKSIDI TË KALLAJIT TË BAZUAR NË STRUKTURA NANOSKOPIKE

JAHJA KOKAJ¹, NEBI ÇAKA², AGON KOKAJ³

¹Department of Physics, Kuwait University, Kuwait

²Faculty of Electrical and Computer Engineering, University of Prishtina, Kosova

³EE Department, College of Engineering and Petroleum, Kuwait University, Kuwait

Email: jkokaj@yahoo.com

ABSTRACT

Tin-oxide thin film is deposited and analyzed using electron microscope, nanoscope and conventional optical techniques. The transmittance and index of refraction against wavelengths is determined using experimental techniques. The properties such as resistivity, mobility and electron concentration are analyzed for this thin-film based semiconductor.

PËRMBLEDHJE

Filmi prej oksidi të kallajit është depozituar dhe analizuar me anë të mikroskopit elektronik, nanoskopit dhe metodave konvencionale optike. Është përcaktuar varësia e indeksit të thyerjes nga gjatësia valore e dritës rënëse, me anë të teknikave ekzistuese eksperimentale. Vetitë e këtij gjysmëpërçuesi apo filmi të hollë, siç janë rezistenca specifike, përqendrimi i elektroneve dhe lëvizshmëria, janë përcaktuar nëpërmes studimit në fjalë.

1. Introduction

Tin oxide is a wide-band gap non-stoichiometric semiconductor with a low n-type resistivity ($\approx 10^{-3} \Omega \text{ cm}$) and high transparency ($\approx 90\%$) in the visible region. The non-stoichiometric resistivity can be reduced to the range of $10^{-4} \Omega \text{ cm}$ by doping, a level suitable for application in thin film solar cells [1, 2]. In addition to solar cell technology, tin oxide has also been used in fabrication of gas sensors due to the sensitivity of its surface conductance to gas adsorption [3, 4]. Fabrication techniques used to deposit tin oxide include dip coating, evaporation, sputtering, chemical vapor deposition (CVD), and spray pyrolysis. Other application, preparation and characterization

techniques and properties of different films have been developed [5-8].

The electrical properties and gas-sensing behavior of SnO_2 films prepared by CVD have been studied [9]. The films were prepared in the temperature range from 300°C to 700°C using direct oxidation of SnCl_4 . The grain sizes increased as the deposition temperature increased and the film had tetragonal retille structure. All films were found to be n-type. However, the electrical properties of the films were largely affected by deposition temperature. As the deposition temperature increased from 300°C to 500°C , film resistivity decreased to $3 \times 10^{-3} \Omega \text{ cm}$, but a further increase of the temperature to 700°C caused a rapid increase in the film resistivity. It was found from Hall measurements that this trend was attributed mainly to carrier concentration rather than carrier mobility. It is concluded that the donor electrons are probably a result of chlorine incorporation into the lattice during the deposition process, with the high resistivity of the 700°C film caused by less Cl content due to the easy decomposition of Sn-Cl bond at high temperatures.

Brown et al. [10] investigated the gas-sensing properties of SnO_2 films. It was shown that high-quality continuous thin films of SnO_{2x} can be produced, are very sensitive to dry CO gas at elevated temperatures. Un-doped films could also be used as rapid humidity sensors up to a few percent RH.

The dependence of structure and morphology of thin SnO_2 films, in particular on the deposition technique was investigated by Popova et al. [11]. The techniques used were CVD, spraying and sputtering. The possibility of utilizing reactive Pulsed Laser Deposition (PLD) with a Sn target and a background oxygen pressure (20 pa)

to form highly transparent and conducting SnO₂ films have been demonstrated [12]. The advantage of this technique is the ease of target preparation and maintenance when compared with using SnO₂ targets. These experiments also suggest that the physical properties of these transparent conducting films can be controlled by proper choice of laser and deposition parameters. For both reactive PLD with Sn targets and PLD with SnO₂ targets, the electrical resistivity of the films was reduced as the substrate temperature during deposition was increased. Films with the lowest resistivity corresponded to a substrate temperature of 400°C.

Tsukuma et al. [13] have used liquid phase deposition for the preparation of SnO₂ films. The films were formed in a solution containing 5-300 mM SnF₂. The procedure of film formation was very simple; the solution, in which a substrate is immersed, is maintained above 40°C for tens of hours. In this method, the hydrolysis product of SnF₂ deposited as the film on a substrate. The tin compounds used in spray pyrolysis solutions have mainly been SnCl₂ [14] and SnCl₄ [15]. Recently, the use of SnF₂ has also been reported [16, 17].

2. Preparation and determination of the sample

For preparation of the sample or deposition of the film we applied spray pyrolysis technique. SnO₂F films were deposited from a solution comprising 23 ml of SnCl₄, 7 ml of H₂O and 920 ml of methanol. Fluorine was added in the form HF instead of NH₄F [2], to give the solution a doping level of F/Sn in the range of 0-180 atomic percent (at %). Since SnCl₄ evaporates easily, it was cooled before and during the solution preparation and was carefully handled under an evacuating chamber. The solution was prepared just before the deposition process. Experimental results will be shown in Section 4.

Deposition system: The deposition system was consisting of an electrical heater, a spray bottle, a chamber, a pump, and an exhaust fan. The heater was equipped with a circular metallic heat sink, on top of which the substrates were placed. The heater was placed over an inclined base through which a tube was connected to the inlet of the exhaust pump; the outlet of the pump was connected to the exhaust fan. The spray bottle had a design similar to that for the Thomas Scientific model 2753-10 with a nozzle diameter of 0.5 mm, and was connected to the carrier gas (pure nitrogen) cylinder through soft tubes. The Chamber was enclosing the heater and has an opening through which the solution was sprayed. The

temperature was monitored by a chromel-alumel thermocouple fixed on top of the heat sink, adjacent to the substrate.

Deposition conditions: Deposition was performed on borosilicate glass substrates at a temperature of 490°C - 525°C and from a distance of approximately 18 cm. The spray rate was ≈ 12 ml/min and the nozzle was scanned over the substrate to ensure uniformity in film thickness. Spraying was done in pulses of approximately 2 s in duration to avoid a substantial fall in the substrate temperature and also to allow the vapor of the sprayed solution, which was forming a cloud over the substrate, to be evacuated through the exhaust. The evacuation rate had to be matched with the spraying rate which, in turn, depends on the diameter of the spray nozzle as well as on the pressure of the carrier gas; otherwise, the spray vapor has a turbulent motion over the substrates, causing non uniform films. To ensure the uniformity of the deposited films, it was also essential to use a heat sink with such a flat surface to give a perfect contact to the substrates. The thickness of the obtained film using known experimental techniques [18] is determined.

Initial measurements: Initial estimates of the thickness of films was obtained from the mass of the deposit using a density of 6.99 g/cm³ [18]. Thickness estimates from the mass deposited and its density is a convenient and proven method which has been applied to many thin solid films including Cu₂O and CdTe. In SnO₂:F films, the possible change of density with heavy doping is negligible since the crystal structure remains the same and the atomic mass of oxygen and fluorine and close to each other. The thicknesses calculated from interference patterns in the transmittance or reflectance spectra of the films using the refractive index of 2.0 reported for SnO₂ at 589.3 nm [16] were in good agreement with our initial estimates.

3. Electron microscopy and nanoscopy

As shown in Fig. 1.a, the film structure we obtained, can not be seen without using microscopy. Due to diffraction limitations where the wavelength plays a key role we could not use a conventional microscope. The grain structure of the film could be seen only by using Electron microscope, as shown in Fig. 1.b.

As is known, the de Broglie wavelength of electrons is much shorter than wave length of any visible color of light. Therefore, we have employed an electron microscope. Using this microscope an image of the film with clear grains on its surface is obtained and is shown in Fig.1. c.

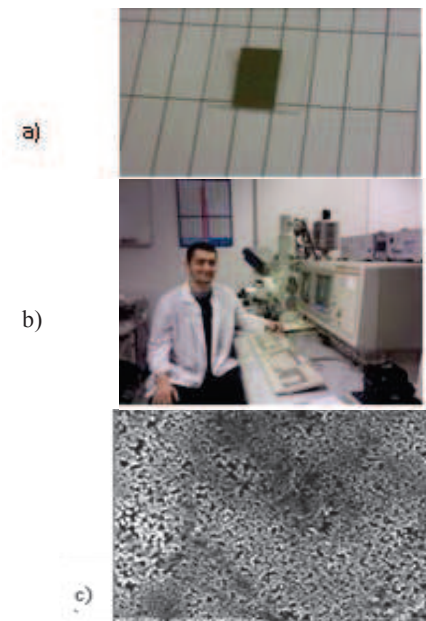


Fig. 1.a) The thin-film based semiconductor (the darker part shown in the middle)

Fig. 1.b) The electron microscope

Fig. 1.c) Grains of the film on the surface obtained by microscope

A further detailed structure of the film is obtained using a nanoscope. In this case there are no diffraction limitations of any kind because the nanoscope has no lens at all. The nanoscope and placement of the film is

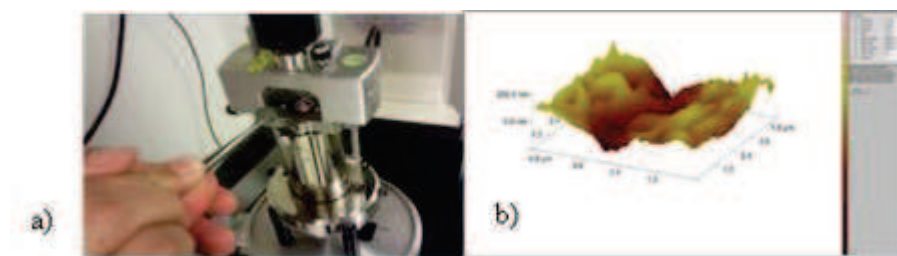


Fig. 2.a) The placement of the film in the lever of the nanoscope.

Fig. 2.b) The 3-D image of the particular part of the surface of the film

The Oxygen deficiency occurs also in films prepared from solutions with much higher O/Sn atomic ratios, possibly due to the effect of methanol [16]. After the initial decrease in n , the electron concentration increases almost linearly with concentration up to F/Sn

shown in Fig. 2. The advantage of the nanoscope is the possibility of obtaining the 3-D image of the film.

The three-dimensional image of the film in the Fig. 2.b is shown. The further studies of the morphology obtained by a ultra small (nanoscopic) vision technology, and quantum mechanical effects related to this small size is a task of our on going work. Here we apply only classical approaches to study some optical properties of the film.

4. Evaluation of Optical Properties (Experimental Results and Discussion)

The doping effect: Films with a thickness in the range of 0.25-0.30 μm were deposited from solutions with different concentration of the dopant. Figure 3 shows the results variation in electrical resistivity (ρ) electron (majority carrier) concentration (n) and electron mobility (μ) with the solution doping level. The resistivity, electron concentration and mobility are measured by using well established techniques [13-17]. As the doping level increases, the resistivity increases initially due to a decrease in n , and then decreases monotonically to $\approx 5 \times 10^{-4} \Omega \text{ cm}$ for F/Sn values greater than $\approx 130 \text{ at.}\%$. The initial decrease in n at F/Sn $\approx 13 \text{ at.}\%$ corresponds to a lower concentration of oxygen vacancies as the result of fluorine incorporation. Although the O/Sn atomic ration in the solution was 2, apparently not all oxygen atoms participate in forming SnO_2 , especially with the reducing effect of methanol which decomposes to CO and H_2 during deposition.

$\approx 90 \text{ at.}\%$ and then saturates at $n \approx 7.5 \times 10^{20} \text{ cm}^{-3}$. SnO_2 has a tetragonal crystal ($a = b = 0.474 \text{ nm}$, $c = 0.319 \text{ nm}$ [18]) and a density of 6.99 g/cm^3 [17]. From these data, it is concluded that for the fluorine-doped films deposited by CVD technique [18, 19]. For

undoped films produced by the CVD technique, $n = 22 \times 10^{19} \text{ cm}^{-3}$, $\mu = 8.5 \text{ cm}^2/\text{Vs}$ and $\rho = 33 \times 10^{-4} \Omega \text{ cm}$, which, except for the mobility, are also comparable with the data shown in Fig. 3.

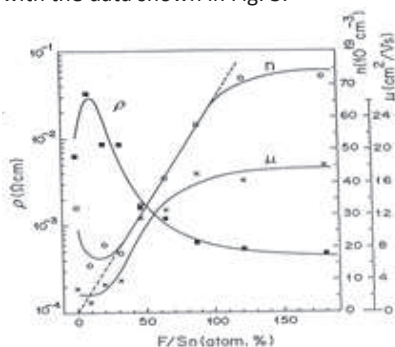


Fig. 3. Variation of film's resistivity (ρ), electron concentration (n) and electron mobility (μ) with doping level in the spray solution.

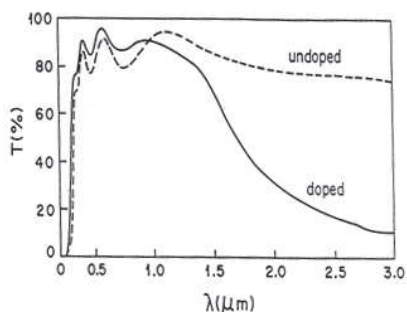


Fig. 4. The transmittance T against wavelength λ for undoped and heavily doped film. For the undoped film $n = 3.2 \times 10^{20} \text{ cm}^{-3}$, $\rho = 63.4 \times 10^{-4} \Omega \text{ cm}$ and thickness is $d = 0.28 \mu\text{m}$.

Dispersion: The transmittance T against the wavelength is measured for two different cases. Figure 4 contains the optical transmittance spectra of the first (un-doped) and the last (heavily doped) sample in the series of samples on which Fig. 3 is based. The average transmittance in the visible region is about 90% for the doped film which has a sheet resistance of $19 \Omega/\square$.

The doped film has a higher transmittance at short wavelengths than the undoped film. This is not because its thickness is slightly smaller. It is mainly due to the effect of doping which improves the transparency as the result of shifting the direct optical transition towards shorter wavelengths. The transmittance of doped film in the near-infrared region indicates an increase in reflectance due to conduction electrons.

5. Summary and Conclusions

Spray-pyrolysis deposition seems to have the best composition, results in high quality films of SnO_2 with optical and electrical properties similar to those for the films deposited by the CVD technique. The sprayed films have even a higher figure of merit for photovoltaic applications. The use of HF as a source for doping is satisfactory. The undoped samples are degenerate with a resistivity in the range of $10^{-3} \Omega \text{ cm}$. This can be lowered by a factor of ≈ 10 by doping. Doping with fluorine enhances the electron mobility and the films transparency at short wavelengths. Dispersion characteristics are described well by the classical bound-electron and free-electron dispersion theories.

LITERATURE

1. J. Britt and C. Ferekides, *Appl. Phys. Lett.* 62, 2851 (1993)
2. S. K. Das and G. C. Morris, *J. Appl. Phys.* 73, 782 (1992)
3. J. Watson, K. Ikohura and G. S. V. Coles, *Mas. Sci. Technol.* 4, 711 (1993)
4. A. L. Dawar and J. C. Joshi, *J. Mater. Sci.* 1 (1984)
5. J. Kokaj et al., *J. Phys. D.* 37, 6 (2004).
6. J. Kokaj et al., *SPIE*, Vol. 3073, 441 (1997)
7. J. Kokaj et al., *Appl. Phys. A*, 89, 923 (2007)
8. A. Rakhshani, J. Kokaj, J. Mathew, B. Peradeep, *B. Appl. Phys. A*, 86, 377, (2007)
9. K. H. Kim and C. G. Park, *J. Electrochem. Soc.*, 138, 8 (1991)
10. J. R. Brown et al., *J. Electrochem. Soc.*, 144, 1 (1997)
11. L. I. Popova, M. G. Michailov, V. K. Gueorguev, *Thin Solid Film* 186, 107 (1990)
12. H. M. Phillips, Y. Li, Z. Bi and B. Zhang, *Appl. Phys. A* 63, 347 (1996)
13. K. Tsukuma, T. Akiyama, H. Imai, *J. Non-Crystalline Solids* 210, 48 (1997)
14. J. F. Jordan and S. P. Albright, *Sol. Cells* 23, 107 (1988)
15. C. Agashe and S. S. Major, *J. Mater. Sci. Letts.* 15, 497 (1996)
16. G. C. Morris and A. E. McElenea, *Appl. Surf. Sci.* 92, 167 (1996)
17. E. Shanthi, V. Dutta, A. Banerjee and K. L. Chopra, *J. Appl. Phys.* 51, 6243 (1980)
18. R. A. Smith, *Semiconductors*, (Cambridge University, Cambridge, 1968), p. 189
19. G. Grosse et al, *Thin Solid Films*, 90, 309 (1982)
20. T. S. Moss, *Optical Properties of the semiconductors*, (Butterworth, London, 1961).